Spikes in Condensed Rare Gases Induced by keV-Atom Bombardment

Herbert M. Urbassek and K. Thomas Waldeer
Institut für Theoretische Physik, Technische Universität, D-3300 Braunschweig, Federal Republic of Germany
(Received 21 January 1991)

We investigate by molecular-dynamics simulation the time evolution of a collision cascade in a condensed Ar solid, initiated by a 1-keV Ar atom. The particle density and velocity in the collision-cascade volume, the kinetic- and potential-energy distributions of the recoiling Ar atoms, and the energy distribution of sputtered particles are monitored. The high pressure building up in the core of the cascade drives the material into the cascade periphery and towards the surface. The surface erupts and hundreds of atoms are emitted, leaving behind a huge crater.

PACS numbers: 79.20.Nc

The consequences of bombarding a strongly bonded material—such as a metal or semiconductor target—with an energetic atom or ion with energies around 1 keV or higher have been well studied in the last decades. Roughly, the following picture has emerged: The bombarding particle dissipates its energy and momentum, via collisions, to the atoms of the target material; these in their turn collide with other target atoms, etc., and thus a *collision cascade* is set up. The displacement processes involved lead to the formation of damage (vacancies and interstitial atoms) in the material, while near-surface atoms which acquire sufficient momentum are emitted (*sputtered*) from the solid. This picture forms the basis of a quantitative theory of damage and sputtering processes,[1] which presupposes that the number of moving atoms in the relevant stages of the process is small (dilute or *linear cascade*).

There may, however, be situations in which essentially *all* target atoms in the collision-cascade volume—or in a near-surface part of it—are set in motion: This then is called a dense cascade or a *spike*. Deviations from the predictions of linear-cascade theory may then be expected, and have been measured using heavy ions and, in particular, molecular ions as projectiles.[2]

Spike effects are particularly drastic when bombarding a volatile solid, such as, e.g., a condensed rare-gas target. For these systems, sputtering yields are measured which are up to an order of magnitude higher than the predictions of linear-cascade theory.[3] While at high emission energies, the energy distribution of sputtered particles follows well the predictions of linear-cascade theory, an abundance of particles emitted below the sublimation energy of the material can be detected.[4,5]

A number of models have been formulated to explain these findings.[6,7] They range from modifications of linear-cascade theory, in which the value and nature of the surface binding energy is changed,[4,8] to the so-called *gas-flow model* which assumes that the high energy density in the cascade volume brings the material above the critical point of the liquid-gas phase transition such that the target atoms are free to flow out into the vacuum above the surface.[3,9] Other models which have been formulated to explain the sputtering from dense cascades comprise the evaporation model, where evaporation from surface regions with high energy density contributes to sputtering,[10,11] and conceptions that a shock wave or pressure pulse originating from the cascade volume can lead to substantial erosion.[12]

In this Letter, we wish to report on the results of a molecular-dynamics simulation of 1-keV Ar bombardment of a condensed Ar target. This specific simulation is able to provide detailed information on the processes occurring in dense cascades and on the mechanisms of sputtering. Previous computer simulations of condensed-gas sputtering were either restricted to very low initial energies,[13] or did not include a sufficient number of target atoms in the simulation.[14]

We model the condensed Ar target as a cubic block of matter of side length 120 Å containing around 42600 Ar atoms. All Ar particles interact with each other via a Lennard-Jones potential with standard parameters,[15] which is smoothly fitted with a KrC potential[16] valid for interaction energies above 1 eV. Electronic excitation and ionization processes are not included in our simulation. In order to allow comparison with linear-cascade predictions, the target has been amorphized; it is cooled down to a temperature of $T_0=0.5$ K. The surface has been allowed to relax freely, while the outermost layers of 9.2 Å of the other five boundaries are coupled to a heat bath of temperature T_0, simulating energy dissipation to the surrounding solid.[17] A highly vectorized molecular-dynamics code is used to calculate the time evolution of the solid upon perpendicular incidence of a 1-keV Ar atom; the Verlet algorithm in velocity form[18] and the neighbor list of Ref. 19 are used. The atomic motion is calculated up to a time of 46 ps after the bombardment and until a distance of 240 Å from the original surface.

The time evolution of the density profile in the irradiated target (Fig. 1) displays how the target material is pressed out of the core of the collision cascade into the periphery and towards the surface. While initially only

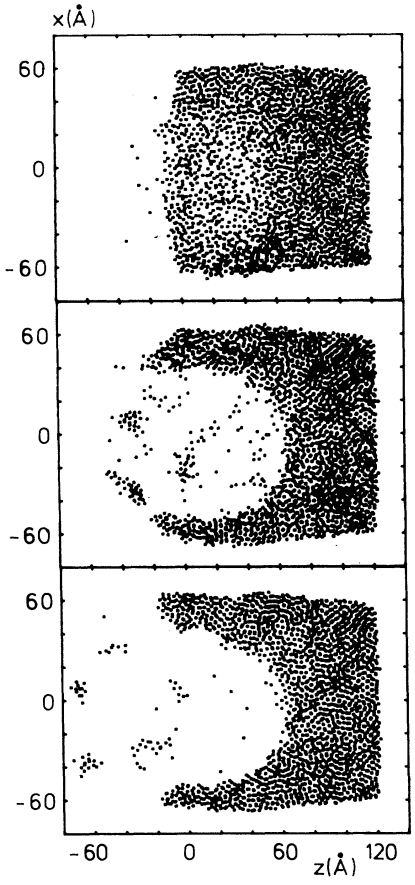

FIG. 1. Time evolution of the density in an amorphous Ar solid irradiated at time $t=0$ at $(x,y,z)=(0,0,0)$ by a 1-keV Ar atom. Every dot represents an Ar atom in a layer extending 3.5 Å on both sides of the plane $y=0$. The surface is initially at $z=0$. Top: $t=3.2$ ps after ion impact. Middle: $t=13.8$ ps. Bottom: $t=24.7$ ps.

some isolated particles are sputtered, eventually, the surface disrupts and a large part of the collision-cascade volume flows out into the vacuum. Finally, a huge crater with dimensions of some 50 Å, surrounded by a rim, is left behind, while atoms and clusters slowly drift away from the surface, and the material in the crater walls has been slightly densified. The velocity profile at an early phase of the expansion process (Fig. 2) clearly indicates the high pressure buildup in the core of the cascade, which leads to a radial, explosionlike expansion of the material. Note the long duration of the process of more than 40 ps. Of course, the situation reached at the last time displayed here is not stable; thermal relaxation and diffusion processes will act to partly heal the surface damage on much longer time scales.

It is important at this point to discuss the potential effects of the boundary conditions in the simulation on the results: We do not fix the outermost atoms; thus we prevent an artificial reflection of the pressure wave from

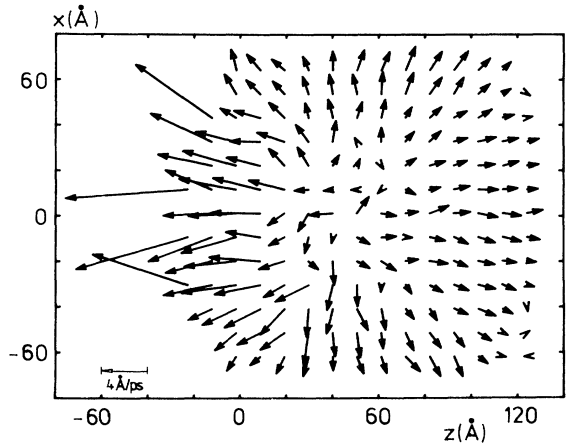

FIG. 2. Velocity distribution corresponding to the earliest plot in Fig. 1. Velocities are calculated as averages over a cubic cell of dimensions $8\times7\times8$ Å^3. Only the projection of the velocities onto the plane $y=0$ is plotted.

the spike at the boundaries. Rather, as evidenced in Fig. 1, the boundaries can yield to the pressure. They do not rupture, though, like the free surface does. A reference calculation at 100-eV Ar impact, where the influence of the boundary conditions on the spike is greatly reduced, shows the same qualitative features as those reported here, but with the crater being of a slightly more conical shape.

The kinetic- and potential-energy distributions of all particles in the simulated volume give further evidence on the nonequilibrium processes occurring under energetic atom bombardment (Fig. 3). Very early after the ion impact, the kinetic energy of most Ar atoms still follows the Maxwell-Boltzmann distribution at $T_0=0.5$ K of the equilibrium solid; additionally a significant number of energized atoms from the early phase of the collision cascade are found. Analogously, the potential-energy distribution peaks heavily at the bulk binding energy of $E_b=0.14$ eV. The shoulder in the distribution represents surface particles which are bound with the surface binding energy $U\cong\frac{2}{3}E_b$, according to their lower coordination number.

After around 3 ps, a drastic nonequilibrium situation has developed. Although there are still particles with very low kinetic energies (at the periphery of the cascade), a high-energy peak at around 50 meV has developed. This energy is somewhat below that corresponding to the critical temperature of the liquid-gas phase transition in Ar, $T_c=151$ K. It is not strictly possible to model the velocity distribution as the superposition of a high- and a low-temperature Maxwell-Boltzmann distribution, though, since it contains excessively many high-energy particles which still did not slow down and thermalize completely in the cascade volume. The potential-energy distribution shows that many parti-

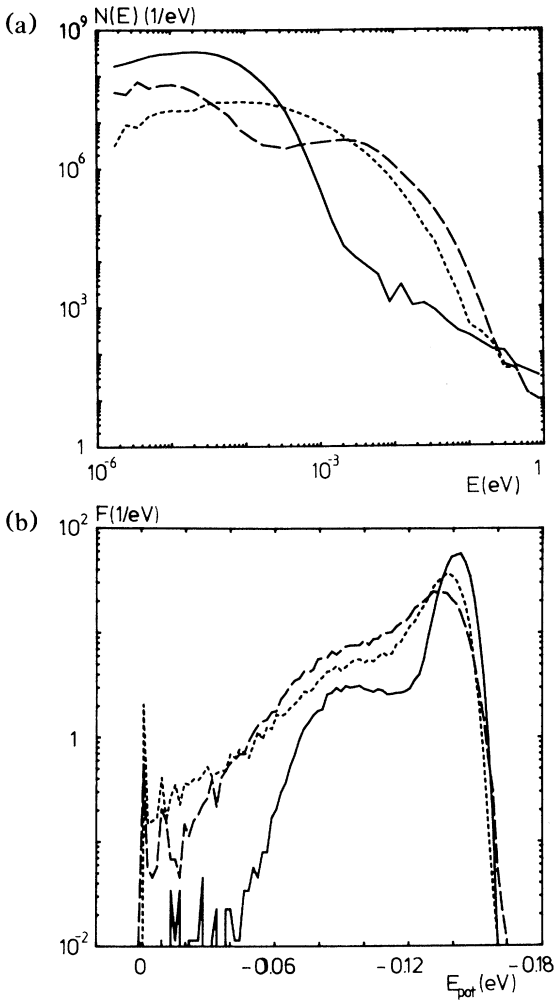

FIG. 3. Time evolution of the (a) kinetic and (b) potential energy of all particles in the simulated volume. Solid line: $t=0.14$ ps after ion impact. Dashed line: $t=3.2$ ps. Dotted line: $t=24.7$ ps.

cles with strongly decreased binding energy exist. These are predominantly particles in the low-density core region of the cascade.

Late after the atom impact, a quasithermal situation was established in the simulated volume. The kinetic-energy distribution is almost Maxwell-Boltzmann at low energies with a temperature of some K only. The potential-energy displays an increased number of weakly bound particles, reflecting the increased surface area in the crater. The peak at $E_{\rm pot}=0$ eV contains the sputtered atoms and the smaller second peak at $E_{\rm pot}=10$ meV contains sputtered atoms bound in dimers.

The kinetic-energy distribution of sputtered particles is shown in Fig. 4 together with results from a simulation[20] based exclusively on linear-cascade theory. Obviously, the high-energy sputtered particles are well described by the assumption of a dilute cascade: These are

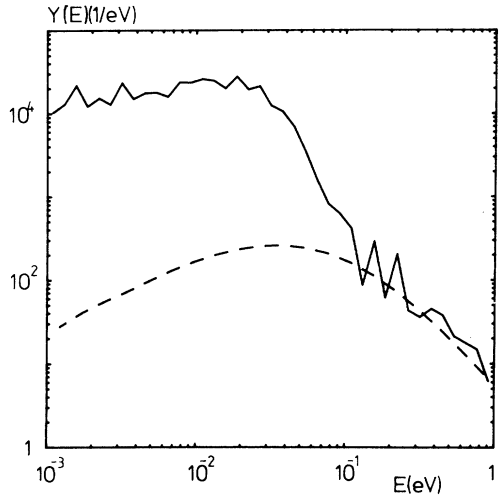

FIG. 4. Energy distribution of all atoms sputtered until 46 ps after the ion impact (solid line). For comparison, the result of a simulation based on linear-cascade theory is also given (dashed line).

the particles sputtered early in the process. Additionally, however, excessively many particles are emitted with energies below the surface binding energy U, with a broad maximum around the critical temperature T_c.

A quantitative comparison to experimental energy distributions is not possible, since no data exist for perpendicular projectile incidence. However, energy distributions of various condensed-gas targets have been measured for oblique ion incidence.[4,5] These all show the above features: a high-energy tail following the E^{-2} decay in agreement with linear-cascade theory, and an excess of very-low-energy particles.

Above, we presented results for an individual ion impact. In order to obtain enough statistics, we simulated a total of 100 events.[21] The average simulated sputter yield until a time of 46 ps after the atom impact is 240 $\pm$ 35 atoms. This is somewhat smaller than the measured yield of 412 ± 40 atoms.[22] We assume the underestimation stems from the influence of the heat-conducting boundaries, which cool the collision cascade volume. We note, however, that fluctuations do exist and are large: The distribution of sputtering yields is very skewed, showing a maximum for yields below 50 atoms, and extending to more than 1000 atoms sputtered. The variance of the simulated yield distribution is 350 atoms. The event presented here has a sputter yield of 911 atoms. It was selected for presentation in order to show dense cascade effects most clearly.

In conclusion, our simulation shows that the high energy density and the large pressure building up in the course of the collision cascade can lead to an explosion-like disruption of the target surface, followed by the jet-like outflow of the hot, weakly bound gas into the vacuum. The process is of long duration, of the order of tens

of ps. The coherent outflow of matter, the long duration of the process, and the definite tendency of forming clusters in the expansion clearly rule out the linear-cascade picture of sputtering or its modifications, as well as surface evaporation. Rather, the process is reminiscent of the pressure-pulse or gas-flow scenarios described above.

These results are of immediate interest for the sputtering of condensed-gas targets and ices, with applications in astrophysics[23] and matrix isolation spectroscopy.[24] The simple, mechanistic nature of the mechanism discussed above—the explosionlike expansion of a highly energized near-surface region—suggests that it may be relevant for the understanding of sputtering from other volatile systems as well, such as the sputtering of bioorganic samples by MeV ions.[12] In strongly bound systems, analogous phenomena have been discussed under the heading of shock-wave or hydrodynamical models.[2]

We acknowledge support from the Deutsche Forschungsgemeinschaft and the help of J. Schüle in the vectorization of our code.

[1]*Sputtering by Particle Bombardment I,* edited by R. Behrisch, Topics in Applied Physics Vol. 47 (Springer-Berlin, 1981); *Sputtering by Particle Bombardment II,* Topics in Applied Physics Vol. 52 (Springer, Berlin, 1983).

[2]P. Sigmund, Nucl. Instrum. Methods Phys. Res., Sect. B **27**, 1 (1987), and references therein.

[3]H. M. Urbassek and J. Michl, Nucl. Instrum. Methods Phys. Res., Sect. B **22**, 480 (1987).

[4]R. A. Haring, R. Pedrys, A. Haring, and A. E. de Vries, Nucl. Instrum. Methods Phys. Res., Sect. B **4**, 40 (1984); B **6**, 585 (1985).

[5]R. Pedrys, Nucl. Instrum. Methods Phys. Res., Sect. B **48**, 525 (1999).

[6]W. L. Brown and R. E. Johnson, Nucl. Instrum. Methods Phys. Res., Sect. B **13**, 295 (1986).

[7]J. Schou, Nucl. Instrum. Methods Phys. Res., Sect. B **27**, 188 (1987).

[8]D. J. O'Shaughnessy, J. W. Boring, J. A. Phipps, and R. E. Johnson, Surf. Sci. **203**, 227 (1988).

[9]D. E. David, T. F. Magnera, R. Tian, and J. Michl, Radiat. Eff. **99**, 247 (1986).

[10]P. Sigmund and C. Claussen, J. Appl. Phys. **52**, 990 (1981).

[11]R. E. Johnson, Int. J. Mass Spectrom. Ion Proc. **78**, 357 (1987).

[12]R. E. Johnson, B. U. R. Sundqvist, A. Hedin, and D. Fenyö, Phys. Rev. B **40**, 49 (1989).

[13]S. T. Cui, P. T. Cummings, and R. E. Johnson, Surf. Sci. **22**, 491 (1989).

[14]B. J. Garrison and N. Winograd, Chem. Phys. Lett. **97**, 381 (1983).

[15]J.-P. Hansen and L. Verlet, Phys. Rev. **184**, 151 (1969).

[16]W. D. Wilson, L. G. Haggermark, and J. P. Biersack, Phys. Rev. B **15**, 2458 (1977).

[17]Y. Wu and R. J. Friauf, J. Appl. Phys. **65**, 4714 (1989).

[18]D. Heermann, *Computer Simulation Methods in Theoretical Physics* (Springer, Berlin, 1990).

[19]G. S. Crest, B. Dünweg, and K. Kremer, J. Comp. Phys. Commun. **55**, 269 (1989).

[20]M. Vicanek and H. M. Urbassek, Nucl. Instrum. Methods Phys. Res., Sect. B **30**, 507 (1988).

[21]K. T. Waldeer and H. M. Urbassek (to be published).

[22]V. Balaji, D. E. David, T. F. Magnera, J. Michl, and H. M. Urbassek, Nucl. Instrum. Methods Phys. Res., Sect. B **46**, 435 (1990).

[23]L. J. Lanzerotti, Nucl. Instrum. Methods Phys. Res., Sect. B **32**, 412 (1988).

[24]J. Michl, Int. J. Mass Spectrom. Ion Proc. **53**, 255 (1983).